Chin. Sci. Bull. (2014) 59(5–6):554–562
DOI 10.1007/s11434-013-0084-6

csb.scichina.com
www.springer.com/scp

Article

Geography

Urban structure and the risk of influenza A (H1N1) outbreaks in municipal districts

Hong Xiao · Xiaoling Lin · Gerardo Chowell · Cunrui Huang · Lidong Gao · Biyun Chen · Zheng Wang · Liang Zhou · Xinguang He · Haining Liu · Xixing Zhang · Huisuo Yang

Received: 3 June 2013 / Accepted: 3 July 2013 / Published online: 17 January 2014

Abstract Changsha was one of the most affected areas during the 2009 A (H1N1) influenza pandemic in China. Here, we analyze the spatial–temporal dynamics of the 2009 pandemic across Changsha municipal districts, evaluate the relationship between case incidence and the local urban spatial structure and predict high-risk areas of influenza A (H1N1). We obtained epidemiological data on all cases of influenza A (H1N1) reported across municipal districts in Changsha during period May 2009–December 2010 and data on population density and basic geographic characteristics for 239 primary schools, 97 middle schools, 347 universities, 96 malls and markets, 674 business districts and 121 hospitals. Spatial–temporal K functions, proximity models and logistic regression were used to analyze the spatial distribution pattern of influenza A (H1N1) incidence and the association between influenza A (H1N1) cases and spatial risk factors and predict the infection risks. We found that the 2009 influenza A (H1N1) was driven by a transmission wave from the center of the study area to surrounding areas and reported cases increased significantly after September 2009. We also found that the distribution of influenza A (H1N1) cases was associated with population density and the presence of nearest public places, especially universities (OR = 10.166). The final predictive risk map based on the multivariate logistic analysis showed high-risk areas concentrated in the center areas of the study area associated with high population density. Our findings support the identification of spatial risk factors and high-risk areas to guide the prioritization of preventive and mitigation efforts against future influenza pandemics.

Keywords Influenza A (H1N1) · Spatial risk factors · Spatial–temporal K functions · Proximity model · Logistic regression

Hong Xiao, Xiaoling Lin and Gerardo Chowell have contributed equally to this work.

H. Xiao (✉) · X. Lin · L. Zhou · X. He · H. Liu
College of Resources and Environment Science, Hunan Normal University, Changsha 410081, China
e-mail: xiaohong.hnnu@gmail.com

G. Chowell
Mathematical, Computational and Modeling Sciences Center, School of Human Evolution and Social Change, Arizona State University, Tempe, AZ 85287, USA

G. Chowell
Division of International Epidemiology and Population Studies, Fogarty International Center, National Institutes of Health, Bethesda, MD 20892, USA

C. Huang
Centre for Environment and Population Health, School of Environment, Griffith University, Brisbane, QLD 4111, Australia

L. Gao · B. Chen
Hunan Provincial Center for Disease Control and Prevention, Changsha 410002, China

Z. Wang
Department of Respiratory and Critical Care Medicine, Beijing Institute of Respiratory Medicine, Beijing Chaoyang Hospital Affiliated to Capital Medical University, Beijing 100020, China

X. Zhang
Changsha Municipal Center for Disease Prevention and Control, Changsha 410001, China

H. Yang
Center for Disease Control and Prevention of Beijing Military Region, Beijing 100042, China

1 Introduction

The 2009 A (H1N1) influenza pandemic was caused by a new triple-reassortant swine-origin influenza virus which was first discovered in North America and Mexico in April 2009 and rapidly spread around the world within weeks [1, 2]. A total of 18,449 laboratory-confirmed A (H1N1) pandemic deaths were reported globally during April 2009–August 2010 (www.who.int/csr/don/2010_08_06/en/index.html). Although a few quantitative studies have analyzed the spatial–temporal patterns of mortality and transmission characteristics of influenza A (H1N1) and other respiratory diseases [3–6], little is known about spatial transmission characteristics of seasonal and pandemic influenza in densely populated urban areas [7].

The accelerated urbanization trends associated with a continuous shift in human populations from rural to densely populated urban areas are changing global patterns of morbidity and mortality [8, 9], especially in the developing countries. In fact, the proportion of the world's population living in urban areas exceeded 50 % in 2008. Moreover, the United Nations has projected that the world's urban population will almost double from 3.3 billion in 2007 to 6.3 billion in 2050 [10, 11]. In China, the total floating population was close to 230 million in 2011, accounting for 17 % of the total population [12]. Also, a higher fraction of the Chinese population is now living in cities than in the countryside. High population density and an increasing floating population may facilitate transmission of infectious diseases in cities by increasing population contact rates [13]. The 2009 A (H1N1) influenza pandemic generated high transmission rates in China since the identification of the first case on 9 May, 2009 [14].

The 2009 A (H1N1) influenza transmission patterns were influenced by a number of factors including the epidemiology of the influenza virus itself, contact rates, people mobility patterns, climatic conditions, school cycles and social distancing measures (e.g., school closure) [15–19]. In particular, the spatial association between A (H1N1) incidence and the distribution of public spaces (e.g., schools, hospitals) and population density in urban areas has not been systematically studied before, but could prove useful to improve epidemiological surveillance and design effective control intervention strategies [20]. Prior studies have identified early transmission onset and higher transmission potential in confined settings and areas with high population density, such as schools [21–23].

Here, we analyzed the spatial–temporal dynamics of the 2009 A (H1N1) influenza pandemic in Changsha, a political, economic and cultural center with a high number of public spaces and a substantial floating population in China that was significantly affected by the 2009 A (H1N1) pandemic [16]. We focused on increasing our understanding of the association between temporal and spatial development of the 2009 pandemic in this region in relation to the population spatial structure characterized by local population density and the distribution of public spaces.

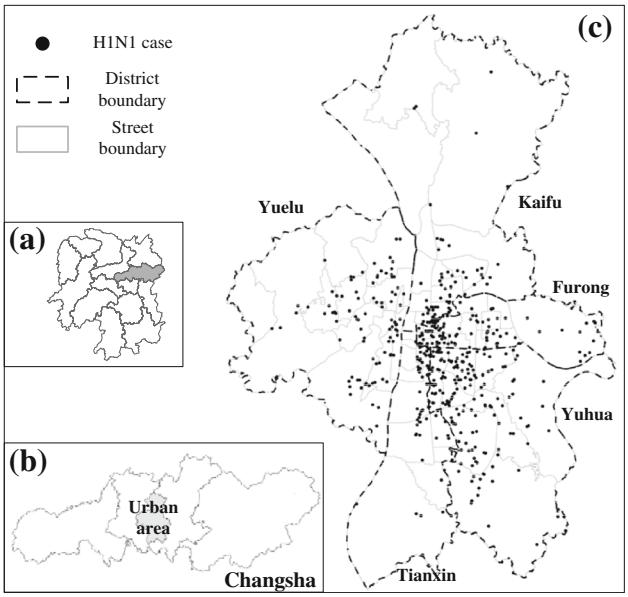

Fig. 1 Study area and the distribution of influenza A (H1N1) cases. **a** Changsha city in Hunan Province; **b** Urban area in Changsha and **c** geographic distribution of influenza A (H1N1) cases based on residential address

2 Materials and methods

2.1 Study area

Changsha, the capital city of the Hunan Province, is located in the northeast region of the province. Changha is about 233 km long and 90 km wide, covering a total land area of 118,000 km^2. Changsha is a political, economic, cultural and traffic center and the most populous city in the Hunan Province, with a population size of 7.04 million in 2010. Moreover, with the accelerated urbanization trends affecting the Changsha–Zhuzhou–Xiangtan city region, all municipal districts of Changsha have experienced a significant increase in their floating population. The urban area of Changsha is comprised by five districts namely Kaifu, Yuelu, Furong, Tianxin and Yuhua. These districts comprise a total of 47 communities, 6 towns and 3 villages (Fig. 1).

2.2 Influenza A (H1N1) cases

We obtained epidemiological information on 1957 A (H1N1) pandemic cases reported across municipal districts of Changsha from May 2009 to December 2010 from the

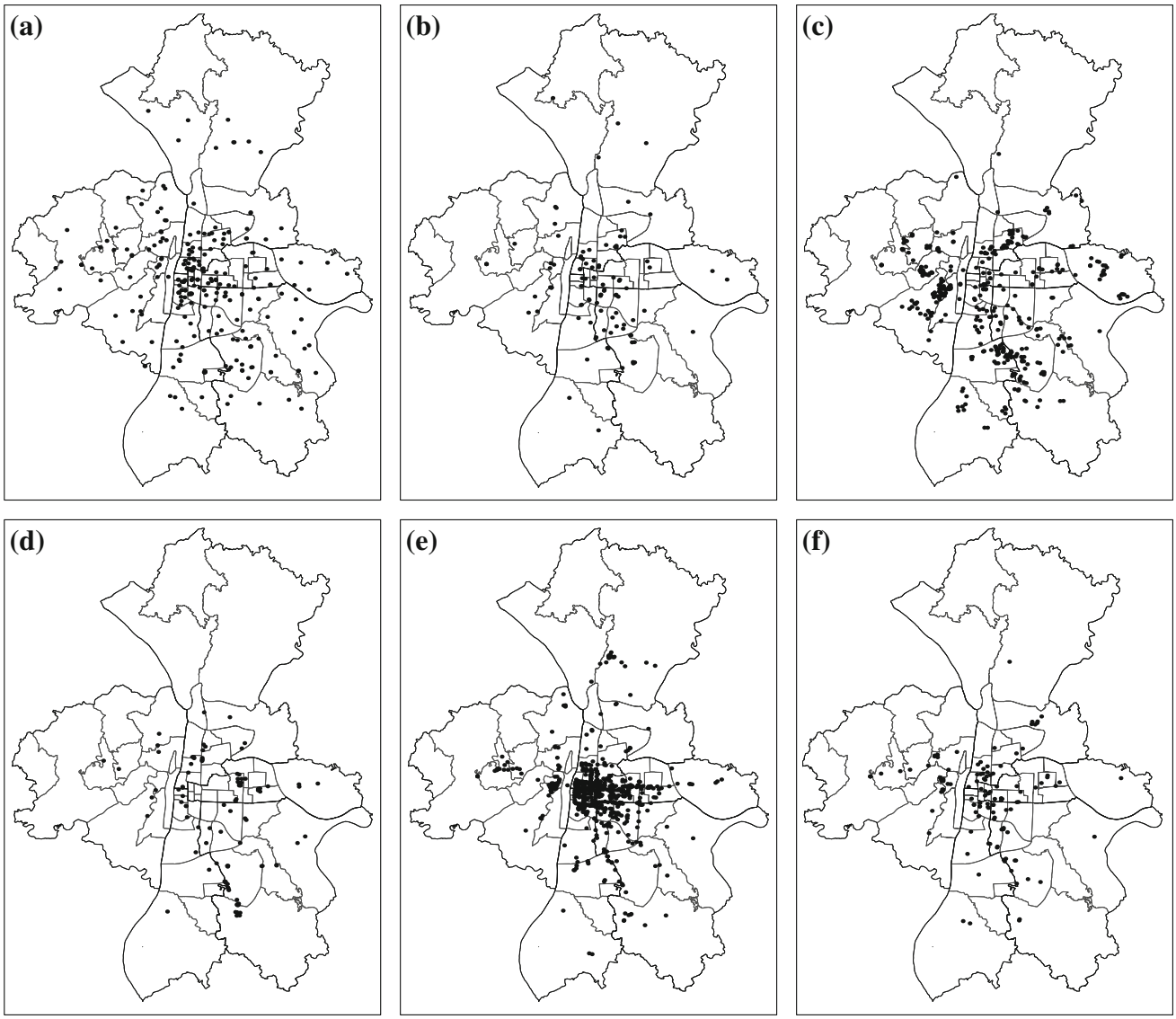

Fig. 2 Distribution of public places: **a** primary schools, **b** middle schools, **c** higher education places, **d** malls and markets, **e** business districts, **f** hospitals

Changsha Center for Disease Control and Prevention (CDC). For each A (H1N1) pandemic case, we obtained gender, age, occupation, residential address and dates of symptoms onset and diagnosis. Each confirmed pandemic (H1N1) influenza case was reported online to the China CDC within 2 h of reporting through a Web-based system that covers all hospitals and clinics in Changsha.

Patients with influenza-like illness (ILI) had sudden onset of fever greater than 38 °C, cough or sore throat, and the absence of other diagnoses according to the guidelines of the World Health Organization (http://www.who.int/csr/resources/publications/surveillance/WHO_CDS_CSR_ISR_99_2_EN/en/). ILI patients visiting hospitals or clinics were tested for A (H1N1) influenza by one or more of the following tests: reverse transcriptase PCR, real-time reverse transcriptase PCR, viral culture or a fourfold rise in specific antibodies to pandemic influenza A virus (http://www.moh.gov.cn/zhuzhan/wsbmgz/201304/7d93ebf8422b4f7a9d8da3162bf0dca8.shtml).

2.3 City's geographic data

We obtained geographic characteristics on all public places located in Changsha in 2009 including primary schools, middle schools, higher education places, malls and markets, business districts and hospitals (Fig. 2). For education institutes, we obtained spatial data for 239 primary schools, 97 middle schools and 347 higher education places from the Hunan Province Education Office. In addition, we also obtained spatial information for 96 malls and markets and

674 business districts from the Changsha Urban and Rural Planning Bureau and for 121 hospitals from the Hunan Provincial Center for Disease Control and Prevention. We used Google Earth for geocoding purposes by using the residential address of public places. The geographic dataset was created in ArcGIS 9.3 (Environmental Sciences Research Institute, Redlands, CA).

Population density at street and township level was calculated using a 9 ‰ population sample survey conducted in 2005 and the *Changsha Statistical Yearbook* in 2006 and 2009. Population density was categorized into three levels: low (<50 per hm^2), middle (50–200 per hm^2) and high (>200 per hm^2) by using the following formula:

$$\mathrm{Popden}_{2008} = \left(\frac{\mathrm{Pop}_{2005}}{\mathrm{Pop}'_{2005}} \times \mathrm{Pop}'_{2008}\right) \Big/ \mathrm{Area}, \quad (1)$$

where Popden_{2008} is the estimated population density at the street and township level in 2008, Pop_{2005} is the population at the street and township level from the 9 ‰ population sample survey conducted in 2005 and $\mathrm{Pop'}_{2005}$ and $\mathrm{Pop'}_{2008}$ are the reported population from the *Changsha Statistical Yearbook* in 2006 and 2009. Area corresponds to the area of each spatial unit (at street or township level).

2.4 Spatial–temporal point pattern analysis

Ripley's K function was employed to analyze our spatial A (H1N1) pandemic data as a point process that changes over different spatial and temporal lags. That is, the outcome of this analysis is plotted against a series of increasing lags where a peak value would suggest an outbreak cluster emerging at the scale of the corresponding lag. Ripley's K function is originally defined as follows [24]:

$$\lambda K(\delta) = E(\delta) \quad (2)$$

where $E(\delta)$ is the expected number of events found within certain scale δ, W_{ij} is the adjustment factor of the edge effects and λ is the intensity of the events. Therefore, the spatial–temporal K function, $K(d,t)$, is defined as the expected number of events per unit of area and per unit of time. That is,

$$K(d,t) = \frac{RT}{n^2}\sum_{i=1}^{n}\sum_{j\neq i}\frac{I_{d,t}(i,j)}{W_{ij}}, \quad (3)$$

where R is the total area of the study, T is the time span from the earliest case to the latest case in the dataset, n is the number of observed cases and $I_{d,t}(i,j)$ is an indicator variable that equals 1 whenever the distance and time intervals of case i and j are within d and t, respectively, and equals 0 otherwise. Finally, a test for space–time interaction may be based on this equation:

$$L(d,t) = K(d,t) - K(d)\cdot K(t). \quad (4)$$

2.5 Statistical analysis

We computed the distance between each of the 1,913 reported cases of A (H1N1) influenza and the nearest public places in 2009. We also calculated the proximity function to infer the relationship between the distribution of A (H1N1) influenza cases and the nearest public places.

Based on the frequency distribution of distances from infections to the nearest public places, 1 km was selected as the threshold distance (i.e., assigned 0 (≥1 km) and 1 (<1 km), respectively). Next, 3,826 points were randomly generated and used as "control" sites (two controls/case). Seven types of spatial risk factors (primary school, middle school, higher education places, hospitals, business district, malls and market, and population density) were considered in this study.

Logistic regression was used to quantify the relationship between the distribution of A (H1N1) influenza cases and public places and local population density. Unconditional logistic regression was performed, and odds ratios (ORs) and their corresponding 95 % confidence intervals (CIs) and P values were estimated by using maximum likelihood methods. ORs of the variables involving minimal distances to the nearest primary school, middle school, higher education places, hospitals, business district and malls and market were calculated for a 1-km difference. Population density was stratified into three levels: 0–50, 50–200 and ≥200 per hm^2. Univariate analyses were first conducted to examine the effect of each variable separately. Multivariate analysis was then performed using the set of significant predictor variables based on our univariate analyses (P value of <0.1). Models were also optimized by comparing the −2 log likelihood and Hosmer–Lemeshow goodness of fit. A P value <0.05 was considered statistically significant by using the backward-LR method.

Finally, we generated a risk prediction map based on our multivariate logistic regression analysis and used 44 influenza A (H1N1) cases reported in 2010 as test points. The risk of A (H1N1) influenza for each grid was calculated and classified as high risk, medium risk and low risk according to quartile levels for the predicted prevalence in the predictive map. The average area under the receiver operating characteristic curve (AUC) was used to evaluate the predictive accuracy of the model. All statistical analyses were performed using SPSS (SPSS Inc., Chicago IL, USA).

3 Urban structure and influenza A (H1N1) outbreaks

3.1 Spatial–temporal distribution of H1N1 cases

A total of 1957 A (H1N1) cases were reported from May 22, 2009, to December 31, 2010, with the great majority of

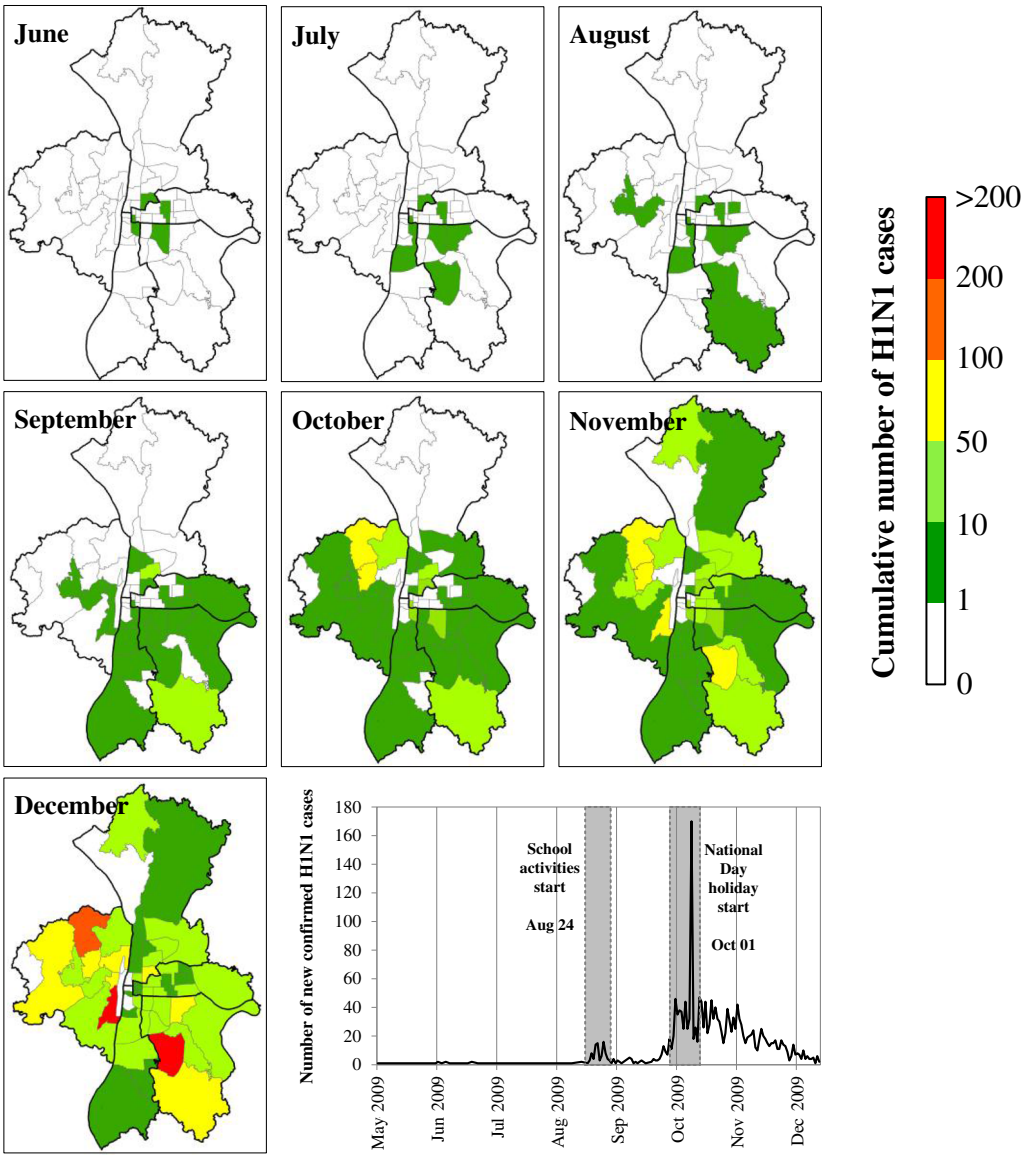

Fig. 3 Monthly distribution of influenza A (H1N1) incidence during outbreaks in 2009. Daily epidemic curve in Changsha urban area, May 22–December 31, 2009, based on laboratory-confirmed A (H1N1) pandemic influenza cases

cases occurring during May–December 2009 (97.8 %). During the initial pandemic phase, there were only scattered reports of 2009 A (H1N1) influenza cases, but the number of cases significantly increased after September 2009 (Fig. 3). A pandemic wave began in September 2009 mainly consisted of students, coinciding with the return of students from summer vacations. The second wave of widespread activity began in October probably influenced by the 1 October National Day holiday, when population movement increases through short- and long-distance travel.

Then number of A (H1N1) cases varied from 85 in the district of Tianxin to 822 cases in the district of Yuelu, while the median number of cases across districts was estimated at 239. The spatial dissemination of influenza A (H1N1) in Changsha appears to have followed a spreading wave from the center to the surrounding areas of the city (Fig. 3). Influenza A (H1N1) cases were rarely reported in the north of the study area, where population density is low and public places are rare. The highest number of influenza A (H1N1) cases were reported in the district of Yuelu.

The spatial–temporal pattern of A (H1N1) reports is illustrated by the spatial–temporal K functions using a contour map (Fig. 4). High values of $L(h)$ in the contour map indicate space–time clustering. The results indicated that the most significant space–time peak involved a time period from 0 to 100 days and a spatial lag from 0 to 5 km. After the initial wave, the second peak involves a time period from 55 to 100 days and a spatial lag from 25 km away.

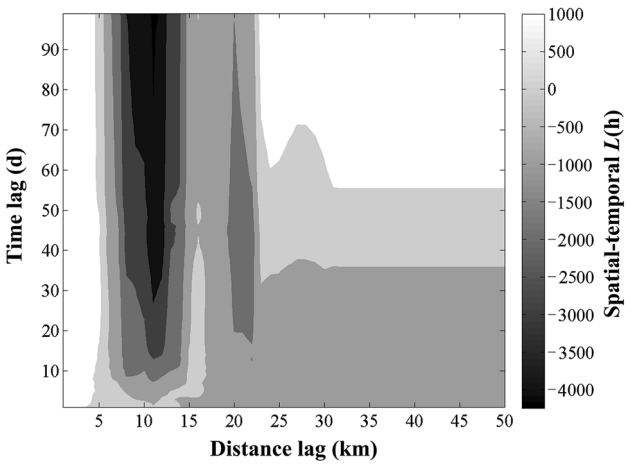

Fig. 4 Contour map of the Spatial–temporal K function. The $L(h)$ is coded from low values, in *black*, to high values, in *white*. The peak value indicates an outbreak cluster emerging at the scale of the corresponding lag

3.2 Distance from A (H1N1) cases to the public places

We found that the distance distribution between A (H1N1) influenza cases and each type of education setting (primary schools, middle schools and higher education places) followed a similar profile (Fig. 5). Correspondingly, the mean distance between A (H1N1) cases and the nearest primary schools, middle schools and higher education places was 0.75 (SD 0.53) km, 1.14 (SD 1.07) km and 0.77 (SD 0.93) km, respectively. However, the corresponding distance profile for the nearest business districts was not unimodal, but showed a skewed distribution with two major peaks occurring at/near <0.2 km and 1.2 km. The mean distance to the nearest malls and markets and the nearest hospitals was estimated at 1.40 (SD 1.44) km and 1.17 (SD 1.11) km (Fig. 5).

3.3 Logistic regression analysis

In our case–control study, minimal distances to the nearest public places and local population density were found to be statistically significant predictors in univariate analyses (Table 1). Moreover, multivariate logistic regression demonstrated that both education places and population density were the most important risk factors influencing influenza A (H1N1) incidence. In particular, the minimum distance to the nearest higher education places was a highly significant risk factor for A (H1N1) incidence (OR = 5.578) (Table 1). Our multivariate logistic regression model was satisfactory as deemed by the average AUC, which was estimated at 0.801.

Based on our predictive model derived from the logistic regression analysis, we generated a predictive risk map of influenza A (H1N1) infections in Changsha using GIS (Fig. 6). The risk of A (H1N1) case events for each grid was classified into three levels: low (<0.3), medium (0.3–0.6) and high (>0.6). Our resulting prediction map indicated that high-risk areas were primarily located in the south-central region, and the risk decayed from the center area to surrounding areas. We also plotted the locations of 44 influenza A (H1N1) cases occurring in 2010, which we used for validation purposes. The overlapping analysis revealed that 90.9 % (40/44) of cases occurred in the predictive high or medium risk areas (Fig. 6). Further, the AUC calculated using influenza A (H1N1) cases in 2010 was estimated at 0.814, confirming the satisfactory performance of our multivariate logistic regression model.

4 Discussion

We have characterized the relationship between pandemic A (H1N1) influenza cases and the population urban structure in Changsha by using spatial–temporal analysis and logistic regression models to identify spatial risk factors. Our results indicate that minimum distance to nearest public places particularly to higher education places (adjusted OR = 5.6) and primary schools (adjusted OR = 1.42) was highly significant risk factors for A (H1N1) influenza. In addition, population density (adjusted OR = 2.8) was also found to be a significant risk factor for A (H1N1) influenza incidence. Our findings indicate that the distribution of public places may affect epidemic development indirectly through its effect on population mixing and flow during daily activity patterns. Findings underscore the need to increase our understanding of the spatial dissemination patterns of A (H1N1) influenza among humans by identifying high-risk areas and related risk factors for infection in urban areas to improve epidemiological surveillance systems and the design of control interventions. This is particularly relevant in the context of delayed vaccine availability during influenza pandemics.

Our analysis of the spatial–temporal distribution pattern of influenza A (H1N1) in Changsha municipal districts showed that A (H1N1) influenza spread from the center of city to surrounding areas, with densely populated areas associated with early transmission events. Further, A (H1N1) influenza incidence increased rapidly after September when students returned to educational activities and A (H1N1) influenza cases mostly consisted of students, which could have amplified transmission as discussed in prior studies [25]. Areas within 5 km from A (H1N1) infections and within 1 km from the nearest public places were associated with high infection risks. However, the distance from infections to the nearest business districts showed a bimodal distribution, indicating two layers of epidemic transmission around business districts

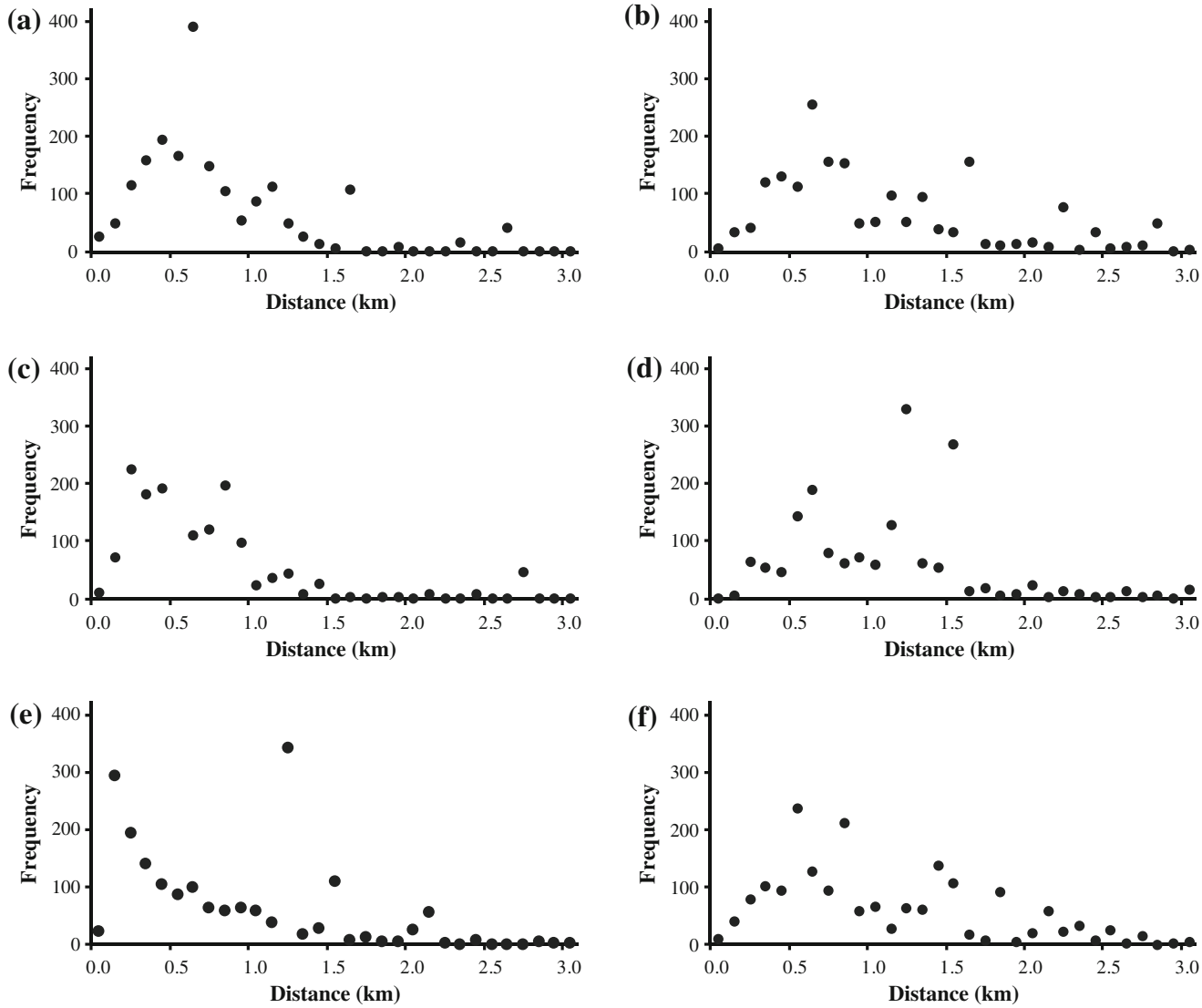

Fig. 5 Frequency distributions of distances from infections to the nearest public places: **a** distance to the nearest primary school, **b** distance to the nearest middle school, **c** distance to the nearest higher education places, **d** distance to the nearest malls and market, **e** distance to the nearest business district, **f** distance to the nearest hospital

(peak-1 = 0.1 km, peak-2 = 1.2 km). Furthermore, infections around malls and market and hospitals were dispersed.

Here, we used the spatial–temporal K functions to depict the spatial–temporal process of A (H1N1) influenza cases. For this purpose, Ripley's K function is an effective approach to quantify point process data with space and time information. However, this analysis alone may bring together irrelevant events that occur too far apart in space or in time to be captured by other means. Our analysis indicated that two clusters occurring during two pandemic waves characterized the diffusion pattern of 2009 influenza A (H1N1) in Changsha's urban area.

High population density areas could facilitate both droplet and aerosol transmission of the influenza virus particularly in confined settings [26]. We found that population density was significantly associated with reports of influenza A (H1N1). Our results support a significant association between population density and transmission of A (H1N1) influenza. Both the A (H1N1) spreading pattern and our predictive risk map showed that high-risk areas concentrated in the central urban area, characterized by high population density.

One previous study found public places (e.g., hospitals, schools) significantly correlated with the incidence rate of severe acute respiratory syndrome in 2003 in Guangzhou [27]. Our logistic regression analysis showed that

Table 1 The association between influenza A (H1N1) outbreaks and spatial risk factors quantified through logistic regression analyses

Influencing factors (units)	Univariate analysis		Multivariate analysis	
	Crude OR[a] (95 % CI)	*P*	Adjusted OR[a] (95 % CI)	*P*
Minimal distances (1 km)				
To the nearest primary school	3.512 (3.103–3.974)	<0.001	1.417 (1.205–1.667)	<0.001
To the nearest middle school	4.715 (4.185–5.312)	<0.001	1.234 (1.046–1.457)	0.013
To the nearest high education places	10.166 (8.795–11.749)	<0.001	5.578 (4.651–6.690)	<0.001
To the nearest hospitals	4.754 (4.217–5.360)	<0.001		
To the nearest business district	2.867 (2.557–3.214)	<0.001		
To the nearest malls and market	2.628 (2.327–2.968)	<0.001		
Population density				
0–50 per hm^2	1.000		1.000	
50–200 per hm^2	6.397 (5.604–7.301)	<0.001	2.798 (2.394–3.270)	<0.001
≥200 per hm^2	8.028 (6.480–9.946)	<0.001	2.704 (2.108–3.469)	<0.001

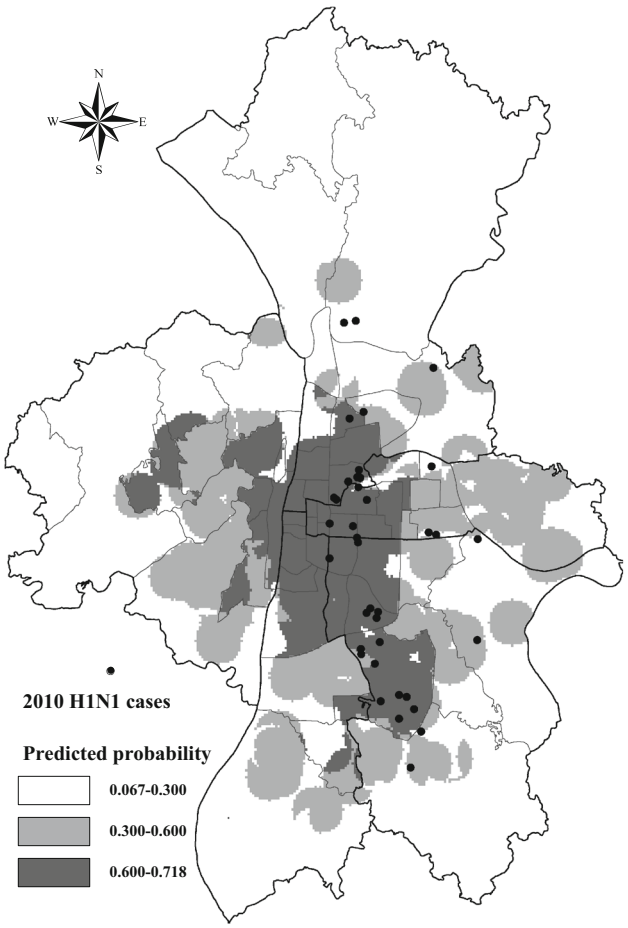

Fig. 6 Predicted risk map overlaid with influenza A (H1N1) cases in 2010

education places are significantly associated as high-risk areas for influenza A (H1N1) outbreaks, which is consistent with the results of prior studies [28, 29]. Influenza transmission is expected to be more frequent between school-aged children as schools play the role of densely populated hubs with high contact rates. In the 2009 influenza A (H1N1) epidemic in Changsha, nearly 79 % cases were students (1515/1913). These results emphasize the need to take adequate prevention measures in school settings [19]. By contrast, the spatial distribution of nearest business districts was not found to be a significant risk factor in our analysis, which could be explained by the distribution of occupations of influenza A (H1N1) cases.

Our study is subject to limitations. Although our study successfully identified statistically significant risk factors associated with influenza A (H1N1) in Changsha, the underlying transmission mechanisms of influenza were not explicitly addressed here. Also, our study was limited to quantifying the association between the distribution of public places and population density and influenza A (H1N1) reports. Hence, further studies could aim to explain spatial influenza incidence patterns in relation to prior immunity patterns and people dynamic contact networks by using spatially explicit mechanistic dynamic transmission models [30, 31].

5 Conclusions

We analyzed the association between the distribution of public places and population density and influenza A (H1N1) reports using detailed spatial data from Changsha, China. We effectively characterized the spatial characteristics of influenza A (H1N1) cases in relation to the spatial distribution of Changsha's urban area in terms of population density and the distribution of public places. This research could motivate the development of predictive capacity for influenza epidemics and pandemics including the design of effective early warning systems and the enhancement of public health measures aimed at containment or mitigation efforts.

Acknowledgments We wish to express our thanks to the anonymous referees for their helpful comments on an earlier draft of this article. This work was supported by the Key Discipline Construction Project in Hunan Province (2008001), the National Natural Science Foundation of China and the Scientific Research Fund of Hunan Provincial Education Department (13A051).

References

1. Garten RJ, Davis CT, Russell CA et al (2009) Antigenic and genetic characteristics of swine-origin 2009 A (H1N1) influenza viruses circulating in humans. Science 325:197–201
2. Viboud C, Simonsen L (2012) Global mortality of 2009 pandemic influenza A H1N1. Lancet Infect Dis 12:651–653
3. Chowell G, Viboud C, Munayco CV et al (2011) Spatial and temporal characteristics of the 2009 A/H1N1 influenza pandemic in Peru. PLoS One 6:e21287
4. Fraser C, Donnelly CA, Cauchemez S et al (2009) Pandemic potential of a strain of influenza A (H1N1): early findings. Science 324:1557–1561
5. Khan K, Arino J, Hu W, Raposo P et al (2009) Spread of a novel influenza A (H1N1) virus via global airline transportation. N Engl J Med 361:212–214
6. Wang JF, Guo YS, Christakos G, Yang WZ, Liao YL, Li ZJ et al (2011) Hand, foot and mouth disease: spatiotemporal transmission and climate. Int J Health Geogr 10:1–10
7. Wang JF, McMichael AJ, Meng B et al (2006) Spatial dynamics of an epidemic of severe acute respiratory syndrome in an urban area. Bull World Health Organ 84:965–968
8. Hay SI, Guerra CA, Tatem AJ et al (2005) Urbanization, malaria transmission and disease burden in Africa. Nat Rev Microbiol 3:81–90
9. Harpham T (1997) Urbanisation and health in transition. Lancet 349(suppl 3):11–13
10. Patel RB, Burke TF (2009) Urbanization—an emerging humanitarian disaster. N Engl J Med 361:741–743
11. Alirol E, Getaz L, Stoll B et al (2011) Urbanisation and infectious diseases in a globalised world. Lancet Infect Dis 11:131–141
12. Department of Floating Population Service and Management of National Population and Family Planning Commission of China. Report on 2012 China's floating population development. Beijing (in Chinese); 2012
13. Lee SS, Wong NS (2011) The clustering and transmission dynamics of pandemic influenza A (H1N1) 2009 cases in Hong Kong. J Infect 63:274–280
14. Cao B, Li XW, Shu YL et al (2009) Clinical and epidemiologic characteristics of 3 early cases of influenza A pandemic (H1N1) 2009 virus infection, People's Republic of China, 2009. Emerg Infect Dis 15:1418–1422
15. Vavricka CJ, Liu Y, Li Q et al (2011) Special features of the 2009 pandemic swine-origin influenza A H1N1 hemagglutinin and neuraminidase. Chin Sci Bull 56:1747–1752
16. Xiao H, Tian HY, Zhao J et al (2011) Influenza A (H1N1) transmission by road traffic between cities and towns. Chin Sci Bull 56:2613–2620
17. Chang CY, Cao CX, Wang Q et al (2010) The novel H1N1 influenza a global airline transmission and early warning without travel containments. Chin Sci Bull 55:3030–3036
18. Xiao H, Tian HY, Lin XL et al (2013) Influence of extreme weather and meteorological anomalies on outbreaks of influenza A (H1N1). Chin Sci Bull 58:741–749
19. Cauchemez S, Ferguson NM, Wachtel C et al (2009) Closure of schools during an influenza pandemic. Lancet Infec Dis 9: 473–481
20. Viboud C, Bjørnstad ON, Smith DL et al (2006) Synchrony, waves, and spatial hierarchies in the spread of influenza. Science 312:447–451
21. Cao ZD, Zeng DJ, Wang QY et al (2010) Epidemiological features and spatio-temporal evolution in the early phase of the Beijing H1N1 epidemic. Acta Geogr Sin 65:361–368 (in Chinese)
22. Chao DL, Halloran ME, Longini IM Jr (2010) School opening dates predict pandemic influenza A(H1N1) outbreaks in the United states. J Infect Dis 202:877–880
23. Vynnycky E, Trindall A, Mangtani P (2007) Estimates of the reproduction numbers of Spanish influenza using morbidity data. Int J Epidemiol 36:881–889
24. Ripley BD (1981) Spatial statistics. John Wiley, New York
25. Yu H, Cauchemez S, Donnelly CA et al (2012) Transmission dynamics, border entry screening, and school holidays during the 2009 influenza A (H1N1) pandemic China. Emerg Infect Dis 18:758–766
26. Tellier R (2009) Aerosol transmission of influenza a virus: a review of new studies. J R Soc Interface 6(Suppl 6):S783–S790
27. Cao ZD, Wang JF, Gao YG et al (2008) Risk factors and autocorrelation characteristics on severe acute respiratory syndrome in Guangzhou. Acta Geogr Sin 63:981–993 (in Chinese)
28. Echevarría-Zuno S, Mejía-Aranguré JM, Mar-Obeso AJ et al (2009) Infection and death from influenza A H1N1 virus in Mexico: a retrospective analysis. Lancet 374:2072–2079
29. Chowell G, Echevarría-Zuno S, Viboud C et al (2011) Characterizing the epidemiology of the 2009 influenza A/H1N1 pandemic in Mexico. PLoS Med 8:e1000436
30. González MC, Hidalgo CA, Barabási AL (2008) Understanding individual human mobility patterns. Nature 453:779–782
31. Apolloni A, Poletto C, Colizza V (2013) Age-specific contacts and travel patterns in the spatial spread of 2009 H1N1 influenza pandemic. BMC Infect Dis 13:176